Sabry.M. AbdelAziz, M.A. Morsy, Mohamed. K. El-Fawkhry

Weldability of super bainitic and triplex structure steels

Welding of super bainitic and triplex structure steels was studied using AWS A5.5 E11018-M and AWS A5.4 E312-17 electrodes. The existence of martensitic structure at the heat affected zone encourages the occurrence of cold cracking at the HAZ in welding of both super bainitic and triplex steels. Using E312-17 electrode renders the occurrence of cold cracks at the heat affected zone of these steels. The tensile strength of welded joints using E11018-M electrode is higher than that of the pure weld metal of E11018-M electrode. This could be attributed to the dilution of weld metal from the base metal especially carbon content. The V– notch impact test results using E312-17 electrode were slightly higher than that obtained using E11018-M electrode. This could be attributed to the occurrence of cold cracks using E11018-M electrode in addition to the tough austenitic weld metal using E312-17 electrode.

1. Introduction

Structural steel is a common category of steel that has been widely used in different purposes. Its chemical composition is varied between high and low alloy containing steel regarding to the applications, the attainable microstructure, and the mechanical properties. Medium carbon steel considers as one of the most reputed grade in the structure steel category, regarding to its heat treatment compatibility. In addition, it has high weldability character, and hot deformation capacity [1, 2].

Carbide free bainitic steels alloyed with high silicon and/or aluminum and high manganese >2%, are reported to achieve an excellent combination of high strength and toughness [3]. Certain content of silicon or aluminum must have been in medium carbon steel to get valid either for super bainitic heat treatment regime or triplex heat treatment regime. It was supposed several percentages of silicon and aluminum to identify the minimum content of silicon or aluminum or the two together to suppress the cementite precipitation. It was found that the minimum content of silicon required to suppress the cementite formation in the medium carbon steel is 0.8%, while it must not exceed 2% regarding to its embrittlement effect [4]. However, the minimum content of aluminum required for suppressing the cementite formation in the medium carbon steel is 0.4%, and the recommended maximum content is 1.2% [5]. Therefore, taking advantage of the ability of silicon and aluminum in suppressing cementite to form cementite free structure with a small fraction of retained austenite, two heat treatment cycles have been established for attaining these odd structures and mechanical properties. One of them aimed at generating bainitic ferrite phase, which contains of laves of carbon supersaturated ferrite interwoven with fine retained austenite. This aimed at forming super bainitic phase (bainitic ferrite and the fineness of retained austenite). While, the second heat treatment cycle aimed at forming of triplex phase (bainite, tempered martensite, retained austenite) [6, 7].

The recent major applications of super bainitic and triplex structure steels are rail way, tank car plate and automotive industry. In welding of high – strength steels, hydrogen- induced cracking or cold cracking problems sometimes force a serious compromise on weld mechanical properties. Typically, this situation arises when post- weld stress relieving cannot be done for any reason to fully safe guard against cold cracking. Consequently, one is forced to carry out welding using soft and ductile filler material [8, 9]. These steels typically have a high carbon equivalent and pose serious cold cracking problems during welding. Standard precautions such as low – hydrogen welding consumables and preheating are not adequate to prevent cold cracking and the selection of austenitic. Austenitic stainless steel fillers are a good choice for them [10, 11]. Due to their high strength level, super bainitic and triplex structure steels can be considered as difficult to weld steels. Therefore, the effect of welding variables on the weldability of these steels are studied to give better insight into the mechanism of attainment of good mechanical properties of the joints using these types of steels.

2. Experimental procedure

2.1. Materials

The base materials used in the current study are four grades of medium carbon steels as plates with dimension of 100 × 100 × 10 mm. The compositions of these grades of steel are given in Table 1. Super bainitc steels can be attained by isothermal heat treatment process by continuous cooling of steel over AC3 to a certain temperature over Ms Temperature (see Figure 1). Triplex structure steels are obtained by isothermal transformation of steel above AC3 to a temperature below Ms, and followed by partitioning and tempering, in order to refine the retained austenite and stress relieve of martensite, respectively (see Figure 1). Two types of shielded metal arc welding electrodes are applied in this research work. The first is a low alloy high strength steel electrode (AWS A5.5 E11018-M) and the second is an austenitic stainless steel electrode (AWS A5.4 E312-17). These electrodes were backed at 350 °C for 2 hours before usage.

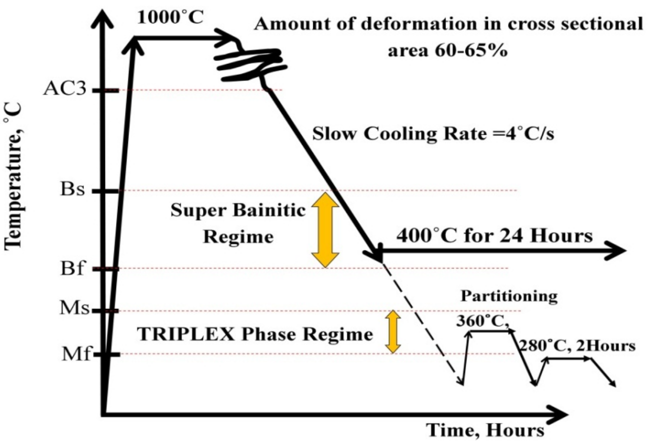

Figure 1: Illustration diagram for the two heat treatment cycles

Steel	Chemical composition, wt %						
	C	Mn	Si	Al	Cr	S	P
A	0.39	2	0.8	0.04	0.58	0.04	0.022
B	0.42	2.08	2	0.45	0.54	0.038	0.029
C	0.41	2.06	0.4	0.4	0.51	0.035	0.025
D	0.45	1.99	0.8	1.2	0.5	0.048	0.024

Table 1: Chemical compositions of the four steel grades, wt %

2.2. Welding variables

The welding parameters are listed in Tables 2 and 3.

Weld metal	Steel grade		Arc welding (A)	Arc voltage (V)	Travel speed (mm/min)	Electrodes polarity	Heat input (kJ/mm)
E11018-M High strength steel	Super bainitic structure steel	A	80	29	74	DCEP	1.6
		B	80	29	79	DCEP	1.5
		C	80	29	70	DCEP	1.7
		D	80	29	66	DCEP	1.8
	Triplex structure steel	A	80	29	79	DCEP	1.5
		B	80	29	76	DCEP	1.55
		C	80	29	68	DCEP	1.75
		D	80	29	79	DCEP	1.5

Table 2: Welding parameters applied in welding of the four steel grades using E11018-M electrode

Weld metal	Steel grade		Arc welding (A)	Arc voltage (V)	Travel speed (mm/min)	Electrodes polarity	Heat input (kJ/mm)
E312-17 austenitic stainless steel	Super bainitic structure steel	A	90	29	89	DCEP	1.5
		B	90	29	102	DCEP	1.3
		C	90	29	92	DCEP	1.45
		D	90	29	95	DCEP	1.4
	Triplex structure steel	A	90	29	78	DCEP	1.7
		B	90	29	89	DCEP	1.5
		C	90	29	89	DCEP	1.5
		D	90	29	95	DCEP	1.4

Table 3: Welding parameters applied in welding of the four steel grades using E312-17 electrode

The heat input is calculated according to the following equation

$$\mathbf{Hi} = \mu \frac{\mathbf{V\,I\,60}}{\mathbf{S\,1000}} \quad \text{........ (kJ/mm)}$$

Where,

Hi: heat input (kJ/mm)

V: arc voltage (volts)

I: current (amps)

S: travel speed (mm/min)

μ: welding heat efficiency (SMAW = 0.85)

2.3. Chemical composition of weld metal and microstructure observation

Chemical compositions of weld metals were analyzed using optical emission spectrometry. After welding cross sections of welded specimens were cut using cooling disk. The cross sections were grinded using abrasive paper starting from 100 mesh to 1000 mesh. Final polishing was conducted to the specimens using alumina past. Etching using 2% Nital solution and a mixture of 10 ml HNO3 + 10 ml acetic acid + 15 ml HCL + 2 – 5 drop glycerin. Microstructure observations have been carried out by using optical and scanning electron microscope.

2.4. Hardness distribution, tensile and V- notch impact tests

Hardness distributions have been carried out by using Vickers hardness testing machine model (DVK – 2 tokoyo japan 1988). Tensile tests have been carried out using tensile machine model (LFM – L 20 KN). V- notch impact tests have been carried out using charpy impact testing machine model (SCHIMADZU No 28093802 – capacity 30 Kg f – made in japan).

3. Results & Discussions

3.1. Chemical compositions of weld metal

Analysis of all weld metal using the two types of electrodes is shown in Table 4.

Element	Chemical composition of Weld metal, wt %	
	E11018-M	E312-17
C	0.0689	0.0822
Si	0.102	1.000
Mn	0.861	0.608
P	0.0208	0.0338
S	0.00912	0.0188
Cr	0.643	27.48
Mo	0.350	0.174
Ni	2.02	11.04
Al	0.00776	0.0113
Co	0.0121	0.172
V	0.00794	0.115
Cu	0.0785	0.242

Table 4: Chemical composition of weld metal, wt %

3.2. Microstructure observations of the specimens, welded using E11018 -M electrode

Figure 2 shows the microstructure of specimen No. A (super bainitic structure steel, 0.8 Si %) that welded using AWS A5.5 E11018 - M electrode. Figure 2a shows the microstructure of base metal. It is a bainitic ferrite phases. Figure 2b and c shows the grain coarsening and grain refinement regions respectively. Grain coarsening region indicated that this region reached to a temperature of 1250

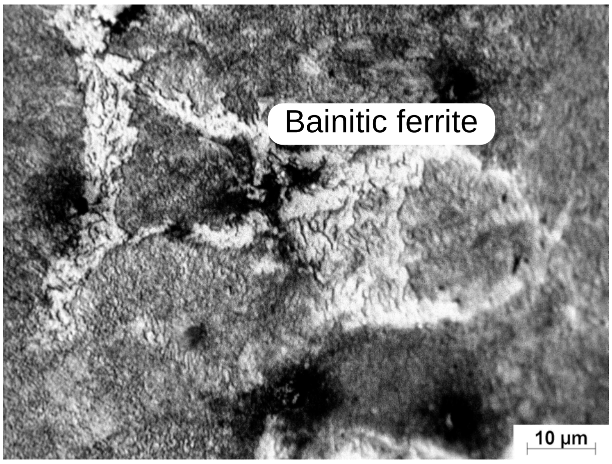

Figure 2a

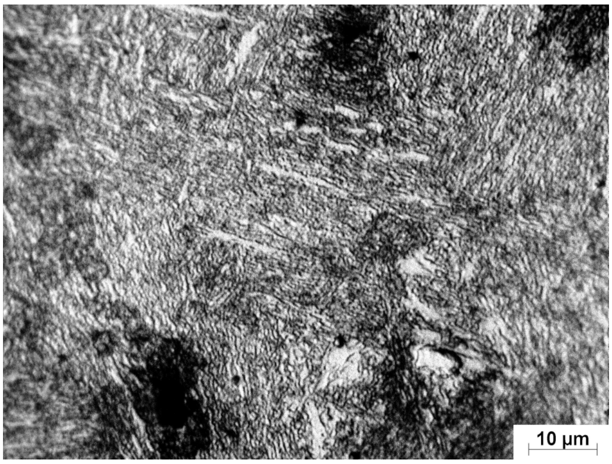

Figure 2b

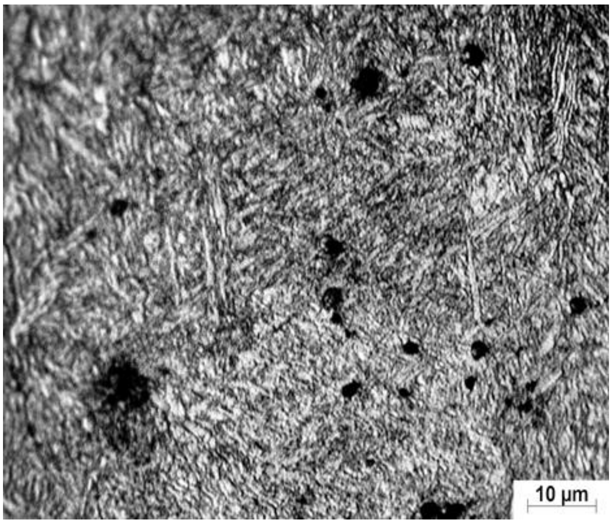

Figure 2c

Figure 2d

Figure 2: Microstructure of joint A welded using E11018-M electrode a) base metal, b) grain coarsening, c) grain refinement and d) weld metal

°C that cause grain coarsening. However, the grain refinement region indicated that this region reached to a temperature of about 900 °C. Figure 2d shows the microstructure of weld metal. It is tempered martensite structure and it is fine microstructure.

Figure 3 shows the microstructure of specimen No. B (super bainitic structure steel, 2 Si %). Figure 3a shows the microstructure of base metal. It is bainitic ferrite microstructure. Figure 3b shows the microstructure of grain coarsening and grain refinement regions. Grain coarsening region indicated that this region reached to a temperature of 1250

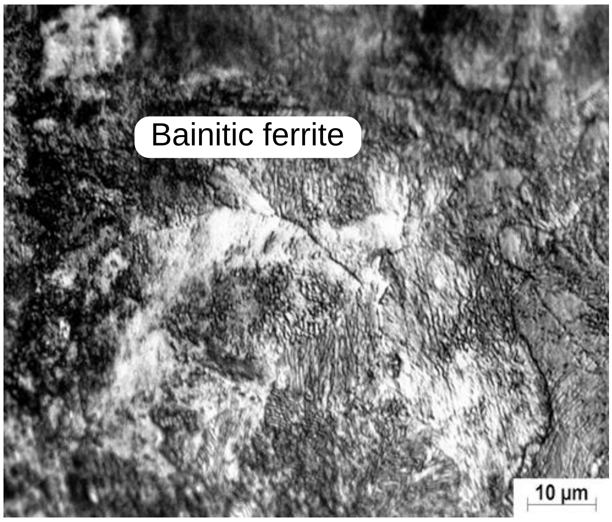

Figure 3a

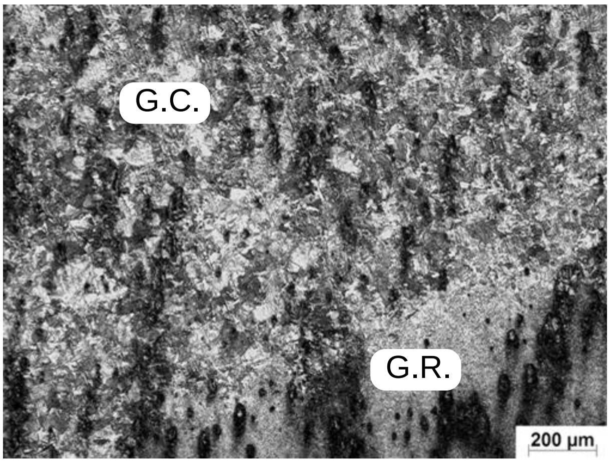

Figure 3b

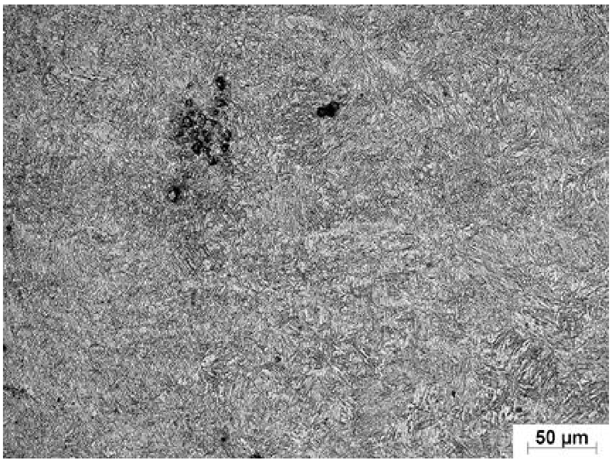

Figure 3c

Figure 3: Microstructure of joint B welded using E11018-M electrode a) base metal, b) grain coarsening and grain refinement, and c) weld metal

°C that cause grain coarsening. However, the grain refinement region indicated that this region reached to a temperature of about 900 °C. Some martensitic structure appeared in the grain coarsening region indicated the high cooling rate of the region. It is tempered martensite structure.

Figure 4 shows the microstructure of specimen No. C (super bainitic structure steel, 0.4 Al %). Figure 4a shows the microstructure of base metal. It is lower bainite and bainite ferrite microstructure. Figure 4b shows the microstructure of grain coarsening and grain refinement regions. Grain coarsening region indicated that this region reached to a temperature of 1250 °C that cause grain coarsening. However, the grain refinement region indicated that this region reached to a temperature of about 900 °C. The grain coarsening regions contain some martensitic structure indicating the high cooling rate of this region. Figure 4c shows the occurrence of crack at the HAZ. The occurrence of this crack may be attributed to the occurrence

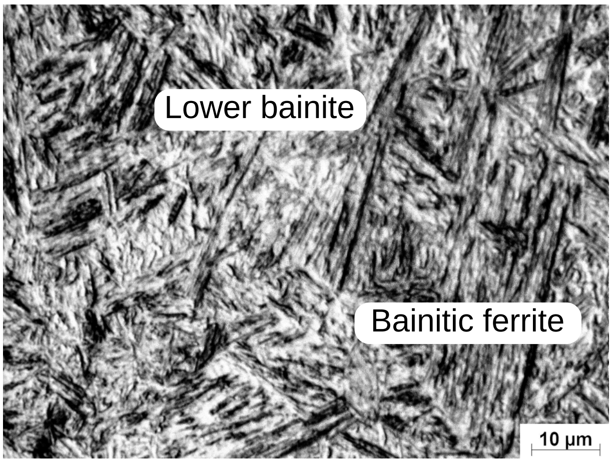

Figure 4a

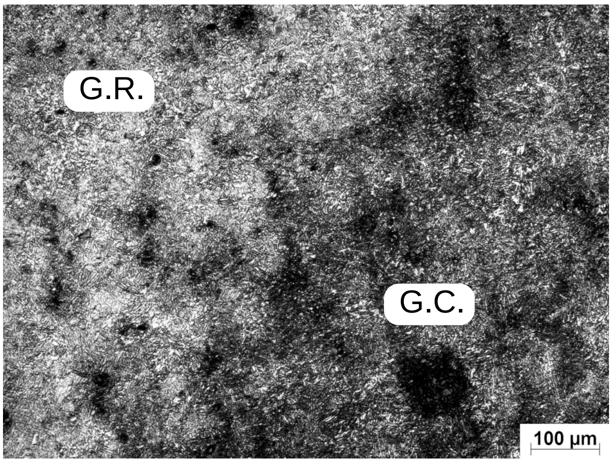

Figure 4b

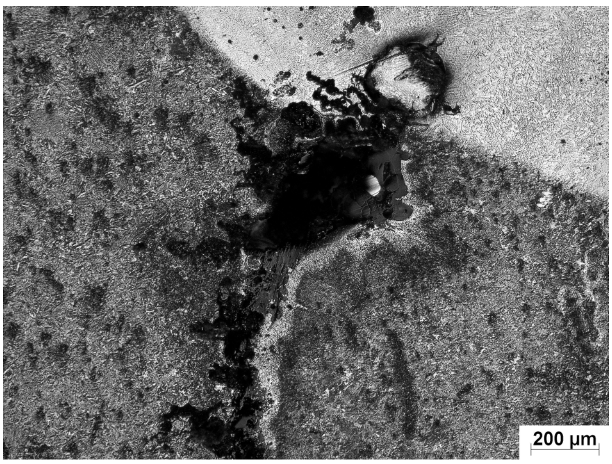

Figure 4c

Figure 4: Microstructure of joint C welded using E11018-M electrode a) base metal, b) grain coarsening and grain refinement, and c) crack in the HAZ region

of cold cracking which occurs due to the formation of martensitic hard microstructure with the existence of diffusible hydrogen and residual stresses.

Figure 5 shows the microstructure of specimen No. D (super bainitic structure steel, 1.2 Al %). Figure 5a shows the microstructure of base metal. It is bainitic ferrite and ferrite phases. Figure 5b shows the microstructure of grain coarsening and grain refinement regions. Grain coarsening region indicated that this region reached to a temperature of 1250 °C that cause grain coarsening. However, the grain refinement region indicated that this region reached to a temperature of about 900 °C. HAZ contain some martensite phases which exist due to high cooling rate. Figure 5c shows the existence of HAZ cracks. This is a cold crack that occurrence as a result of the existence of diffusible hydrogen and the residual stress beside the formation of martensite structure.

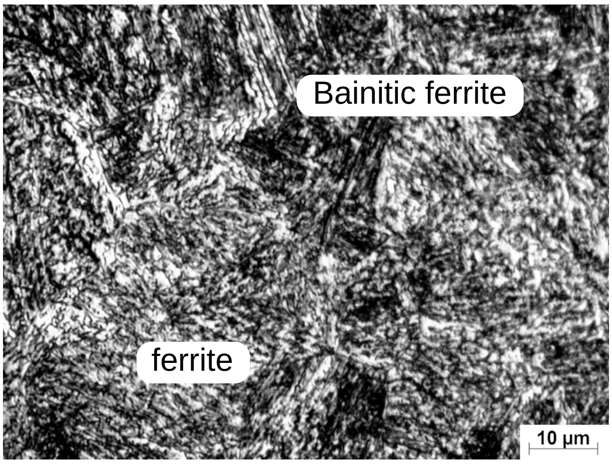

Figure 5a

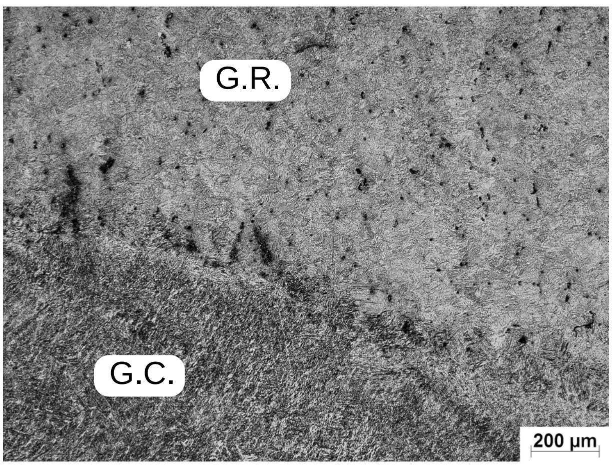

Figure 5b

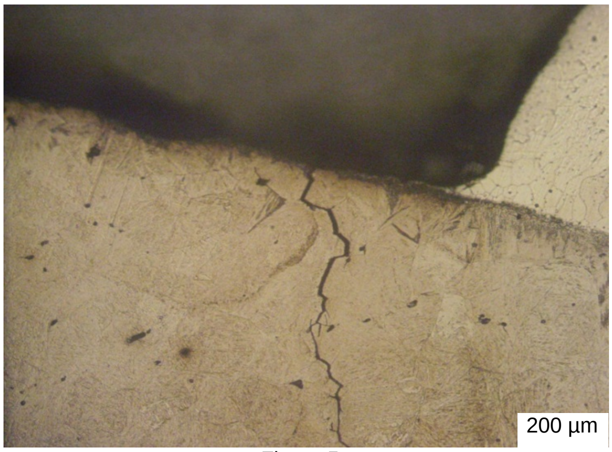

Figure 5c

Figure 5: Microstructure of joint D welded using E11018-M electrode a) base metal, b) grain coarsening and grain refinement, and c) crack in the HAZ region

Figure 6 shows the microstructure of specimen No. A (triplex structure steel, 0.8 Si %) welded using E11018-M electrode. Figure 6a shows the microstructure of base metal. It is fine bainite and acicular ferrite phases. Figure 6b shows the microstructure of grain coarsening and grain refinement regions. Grain coarsening region indicated that this region reached to a temperature of 1250 °C that cause grain coarsening. However, the grain refinement region indicated that this region reached to a temperature of about 900 °C. Figure 6c shows the microstructure of weld metal. It is tempered martensite structure.

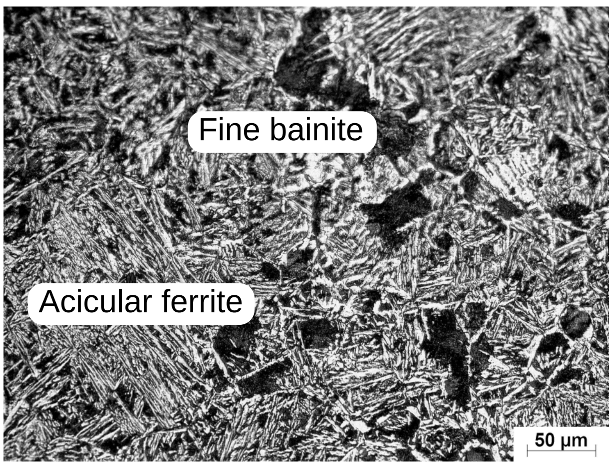

Figure 6a

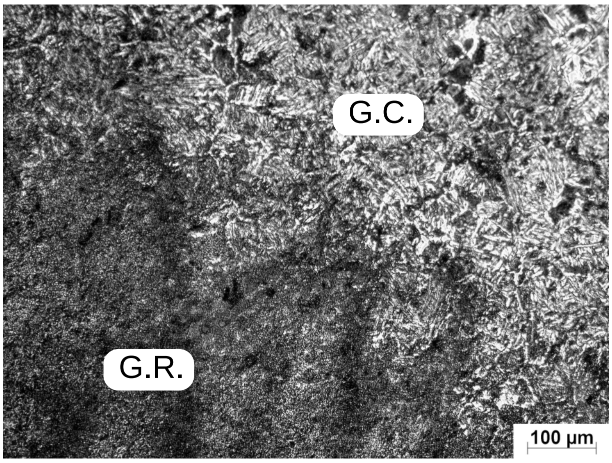

Figure 6b

Figure 6c

Figure 6: Microstructure of joint A welded using E11018-M electrode a) base metal, b) grain coarsening and grain refinement and c) weld metal

Figure 7 shows the microstructure of specimen No. B (triplex structure steel, 2 Si %) welded using E11018-M electrode. Figure 7a shows the microstructure of base metal. It is bainitic ferrite with acicular ferrite and bainite phases. Figure 7b shows the microstructure of grain coarsening and grain refinement regions. Grain coarsening region indicated that this region reached to a temperature of 1250 °C that cause grain coarsening. However, the grain refinement region indicated that this region reached a temperature of about 900 °C. The HAZ also shows the occurrence the crack, the crack occurs as a result of the existence martensitic structure with diffusible hydrogen content and residual stress.

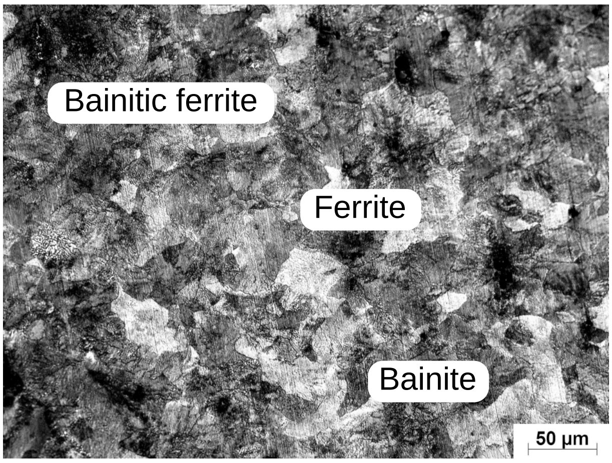

Figure 7a

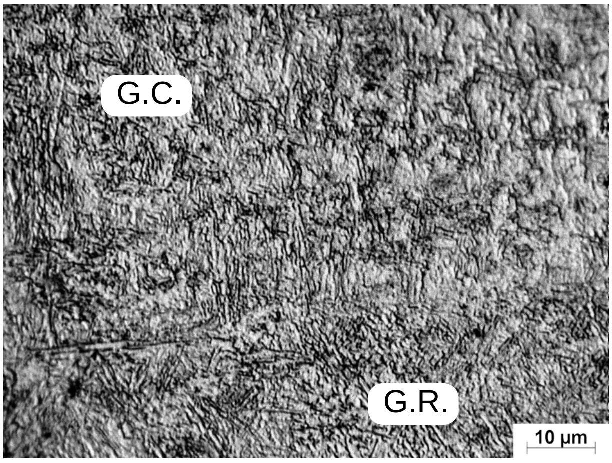

Figure 7b

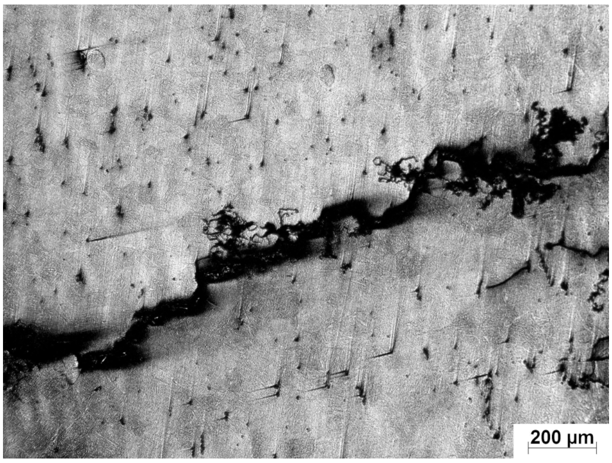

Figure 7c

Figure 7: Microstructure of joint B welded using E11018-M electrode a) base metal, b) grain coarsening and grain refinement, c) crack in the HAZ

Figure 8 shows the microstructure of specimen No. C (triplex structure steel, 0.4 Al %) welded using E11018-M electrode. Figure 8a shows the microstructure of base metal. It is tempered martensite structure with block austenite. Figure 8b shows the heat affected zone. A crack was observed at

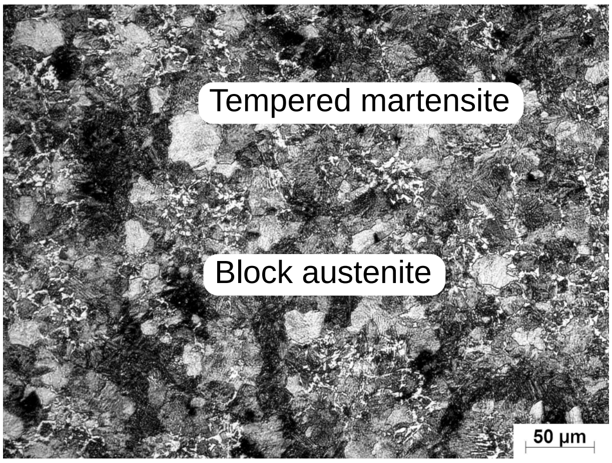

Figure 8a

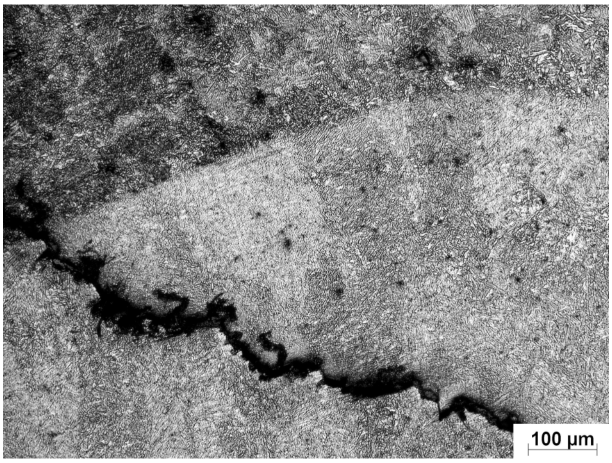

Figure 8b

Figure 8: Microstructure of joint C welded using E11018-M electrode a) base metal, b) the crack in the HAZ

the heat affected zone. It is a cold crack type.

Figure 9 shows the microstructure of specimen No. D (triplex structure steel, 1.2 Al %) welded using E11018-M electrode. Figure 9a shows the

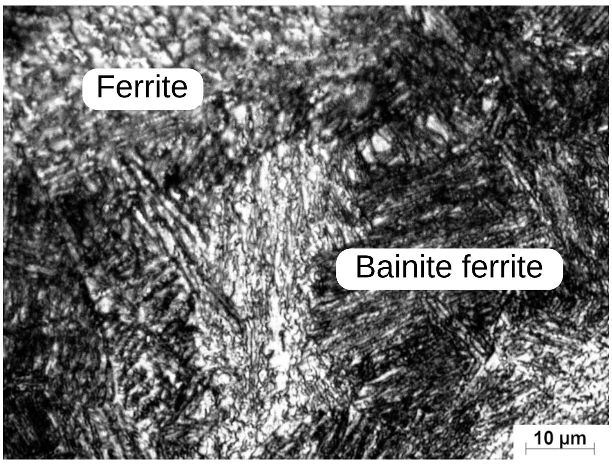

Figure 9a

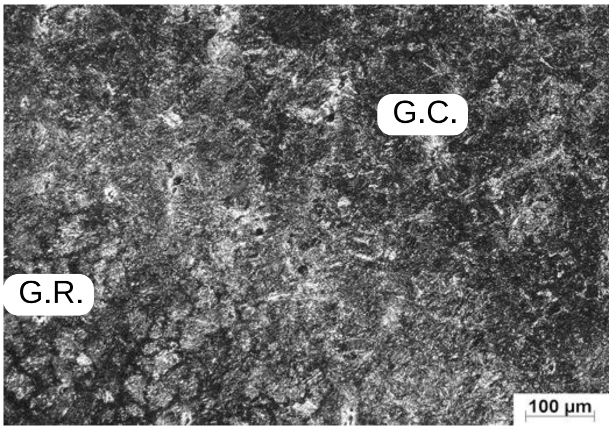

Figure 9b

Figure 9: Microstructure of joint D welded using E11018-M electrode a) base metal, b) No crack in the HAZ

microstructure of base metal. It is ferrite with bainitic ferrite. No crack appearing in the heat affected zone as shown in Figure 9b.

3.3. Microstructure of the joints welded using E312-17 electrode

Steel A that was heat treated to obtain super bainitic structure was welded using E312-17 electrode. Figure 10 shows the microstructure of the HAZ. Cracks not observed using this electrode. Also, welding using E312-17 electrode was applied to steel A that was heat treated to obtain triplex structure. Figure 11 shows the microstructure of the HAZ indicating the disappearance of cracking. Disappearance of cracking in the HAZ of the joints using E312-17 electrode could be attributed to the very low diffusion rate

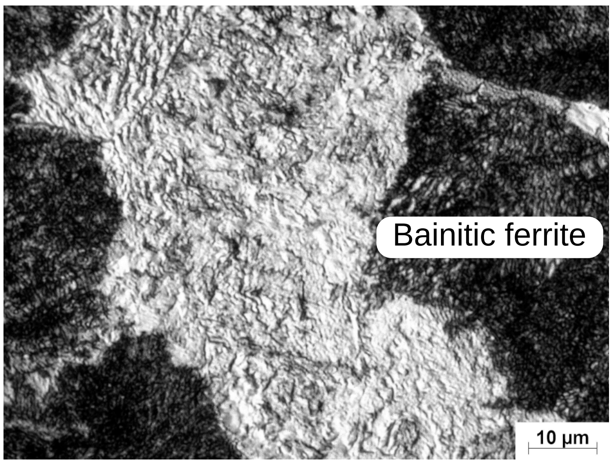

Figure 10a

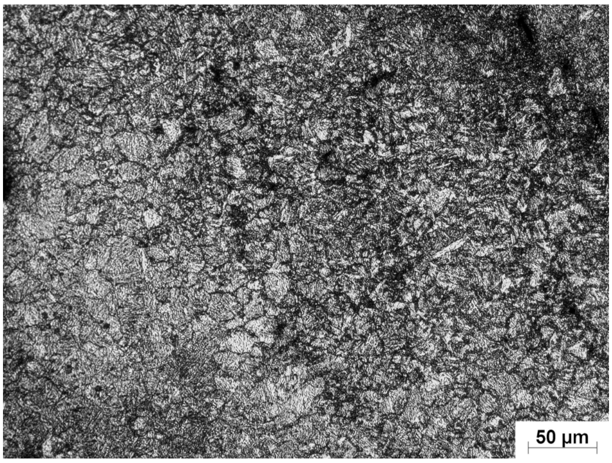

Figure 10b

Figure 10: Microstructure of joint (A super bainitic structure steel) welded using E312-17 electrode a) base metal, b) the HAZ region

of hydrogen in the austenitic microstructure which prevent the existence of diffusible hydrogen in the HAZ and thus render the occurrence of cold crack in the HAZ. Figure 12 shows

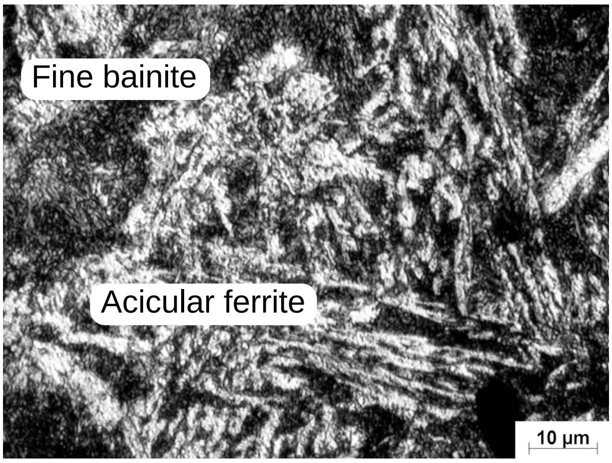

Figure 11a

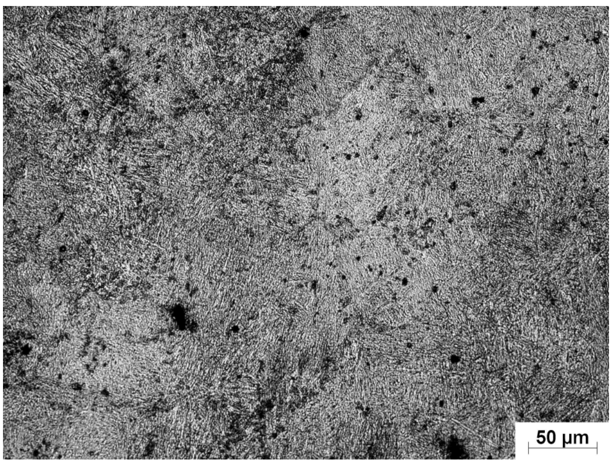

Figure 11b

Figure 11: Microstructure of joint (A triplex structure steel) welded using E312-17 electrode a) base metal, b) the HAZ region

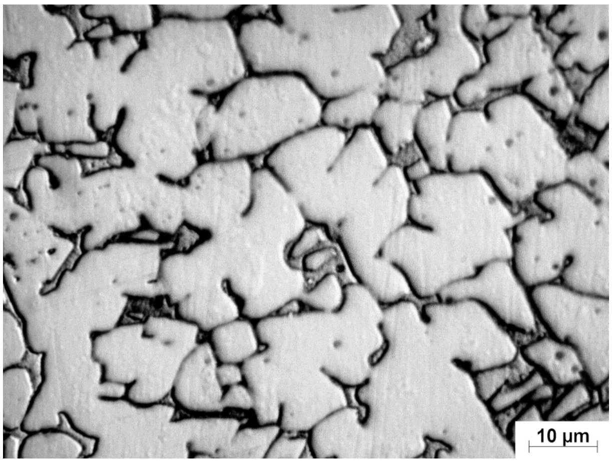

Figure 12: The dendritic structure of austenitic electrode

the dendritic structure of the austenitic electrode weld metal.

3.3. Hardness distribution at the welded joints

Tables 5 and 6 show the hardness levels at the different regions of the welded joint specimens. The very high hardness at the HAZ of specimen B, C and D in super bainitic structure steels and specimens B, C and D in triplex structure steels could be attributed to the high cooling rate and formation of martensitic structure. The high hardness values show the occurrence of cracks using E11018-M electrode. The hardness of E11018-M weld metal is higher than that of the weld metal using E312-17 electrode. Although, the hardness values of the HAZ using both E11018-M and E312-17 electrodes are close to each other, the cracks occur in the HAZ of the base metal using E11018-M electrode only. The diffusion of hydrogen in austenitic stainless steel is negligible compared to its diffusion in E11018-M weld metal and martensitic heat affected zone (HAZ) of base metal. Thus, austenitic weld metal renders the diffusion of diffusible hydrogen in the HAZ of base metal preventing the formation of HAZ cold cracking which occurs due to the simultaneous existence of the martensitic structure, diffusible hydrogen content and the residual stress in the HAZ

Steel Grade		Average Hardness readings, Hv10		
		BM	HAZ	WM
Steel A	super bainitic structure steel after welding using AWS A5.5 E11018-M electrode	351	312	410
Steel B		335	458	415
Steel C		470	431	366
Steel D		410	583	400
Steel A	triplex structure steel after welding using AWS A5.5 E11018-M electrode	288	325	416
Steel B		318	470	412
Steel C		437	460	389
Steel D		395	410	405

Table 5: Hardness values at different locations

Steel Grade		Average Hardness readings, Hv10		
		BM	HAZ	WM
Steel A	super bainitic structure steel after welding using AWS A5.4 E312-17electrode	351	319	278
Steel B		335	460	293
Steel C		470	432	308
Steel D		410	580	299
Steel A	triplex structure steel after welding using AWS A5.4 E312-17electrode	288	325	272
Steel B		318	457	287
Steel C		437	450	270
Steel D		395	407	290

Table 6: Hardness values at different locations

as mentioned in section 3.2.

3.4. Tensile and V- notch impact properties of welded joints

Tables 7 and 8 show the tensile strength of welded joints using E11018-M electrode and E312-17 electrode. Respectively, although the minimum ultimate tensile strength of pure weld metal of E11018-M electrode is about 780 MPa, some of joints fractured at the weld metal at a higher strength level more than this value (1200 MPa). This could be attributed to the dilution of the weld metal from the base metal (mainly carbon content). Analysis of the weld metal at this joint indicating the rise of carbon content from that of the pure weld metal (reached to 0.21 % compared with 0.06 % of pure weld metal). All the joints welded using E312-17 electrode show a fracture located at the weld metal. The same results were attained in welding of armor steels [12]. Thus, prevention of cold cracking by using austenitic E312-17 electrode may result in a sight lowering of welded joint tensile strength [12].

Tables 9 and 10 show the V- notch impact test results using E11018-M and E312-17 electrodes respectively, using E312-17 electrode resulted in tougher weld metal properties than that obtained using E11018-M electrode. The very low values of V- notch impact values of the joints

Steel Grade		Tensile strength of welded joints, MPa	Fracture locations
Steel A	super bainitic structure steel after welding using AWS A5.5 E11018-M electrode	936	HAZ
Steel B		1005	BM
Steel C		1098	WM
Steel D		1200	WM
Steel A	triplex structure steel after welding using AWS A5.5 E11018-M electrode	864	BM
Steel B		954	BM
Steel C		1167	WM
Steel D		1185	BM

Table 7: Tensile strength of welded joints using E11018-M electrode

Steel Grade		Tensile strength of welded joints,MPa	Fracture locations
Steel A	super bainitic structure steel after welding using AWS A5.4 E312-17electrode	834	WM
Steel B		879	WM
Steel C		924	WM
Steel D		897	WM
Steel A	triplex structure steel after welding using AWS A5.4 E312-17electrode	816	WM
Steel B		861	WM
Steel C		810	WM
Steel D		870	WM

Table 8: Tensile strength of welded joints using E312-17 electrode

Steel Grade		Impact test results (J)
		R. Temp.
Steel A	super bainitic structure steel after welding using AWS A5.5 E11018-M electrode	25
Steel B		28
Steel C		18
Steel D		31
Steel A	Triplex structure steel after welding using AWS A5.5 E11018-M electrode	22
Steel B		16
Steel C		15
Steel D		23

Table 9: V- notch impact tests values of welded joints

Steel Grade		Impact test results (J)
		R. Temp.
Steel A	super bainitic structure steel after welding using AWS A5.4 E312-17 electrode	39
Steel B		28
Steel C		28
Steel D		33
Steel A	Triplex structure steel after welding using AWS A5.4 E312-17 electrode	30
Steel B		32
Steel C		28
Steel D		29

Table 10: V- notch impact tests values of welded joints

welded using E11018-M electrode for specimen C (super bainitic), specimen B and C (triplex structure steel) could be attributed to the occurrence of cold crack as shown in Figure 4, 5, 7 and 8 (see section 3.2).

Conclusions

Welding of super bainitic and triplex structure steels using two types of welding electrodes namely AWS 5.5 E11018-M and AWS 5.4 E312-17 electrodes was investigated. The following results were obtained:

• The existence of martensitic structure at the heat affected zone encourages the occurrence of cold cracking at the HAZ in welding of both super bainitic and triplex steels.

• Using E312-17 electrode renders the occurrence of cold cracks at the heat affected zone of these steels.

• The tensile strength of welded joints using E11018-M electrode is higher than that of the pure weld metal of E11018-M electrode. This could be attributed to the dilution of weld metal from the base metal especially carbon content.

• The V– notch impact test results using E312-17 electrode were slightly higher than that obtained using E11018-M electrode. This could be attributed to the occurrence of cold cracks using E11018-M electrode in addition to the tough austenitic weld metal using E312-17 electrode.

Appendix

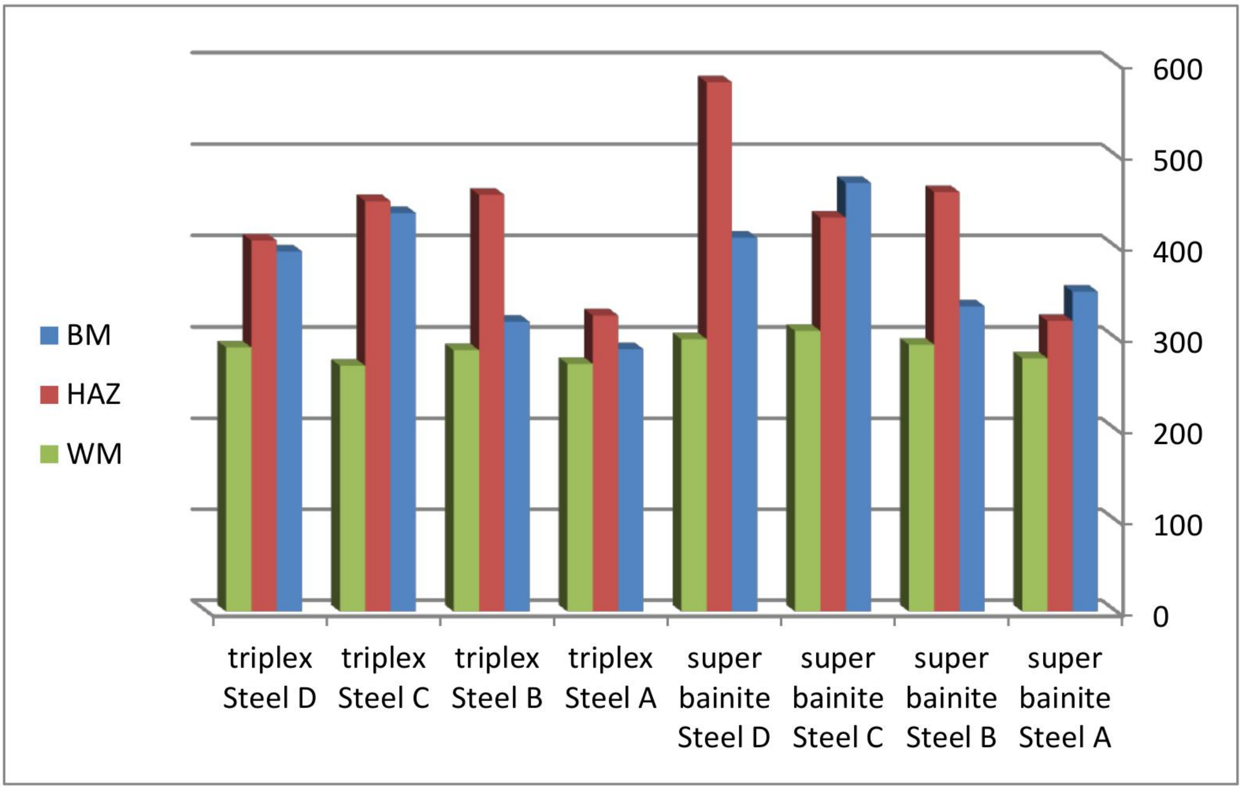

Figure 13: Histogram of hardness value at different location for super bainitic and triplex structure steels after welding using E11018-M electrode

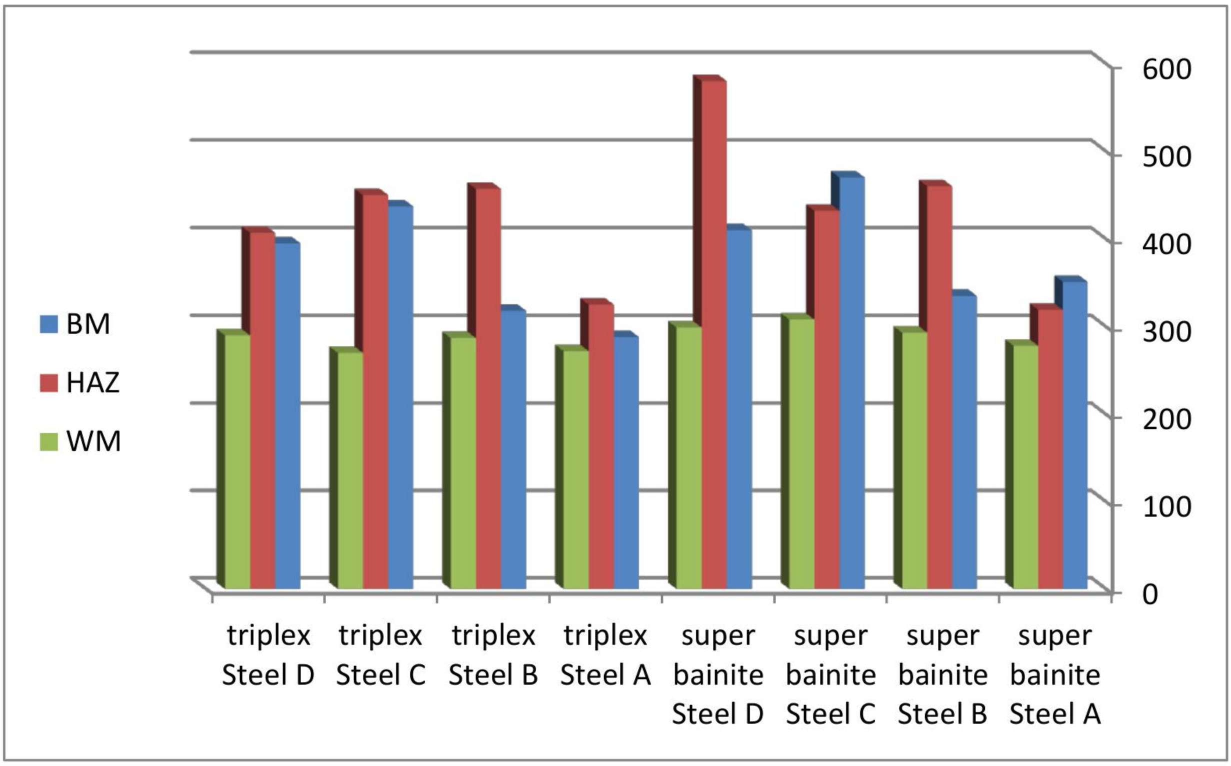

Figure 14: Histogram of hardness value at different location for super bainitic and triplex structure steels after welding using E312-17 electrode

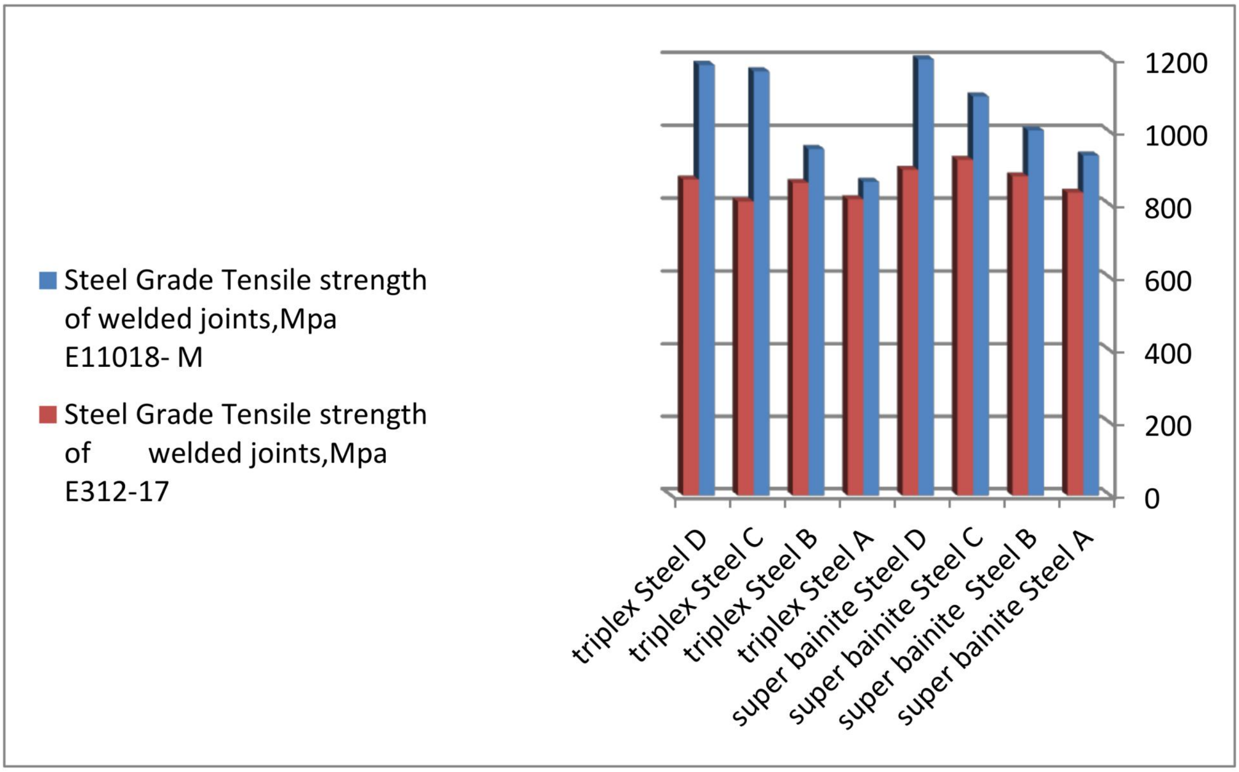

Figure 15: Histogram of tensile of welded joints super bainitic and triplex structure steels after welding using E11018-M and E312-17 electrodes

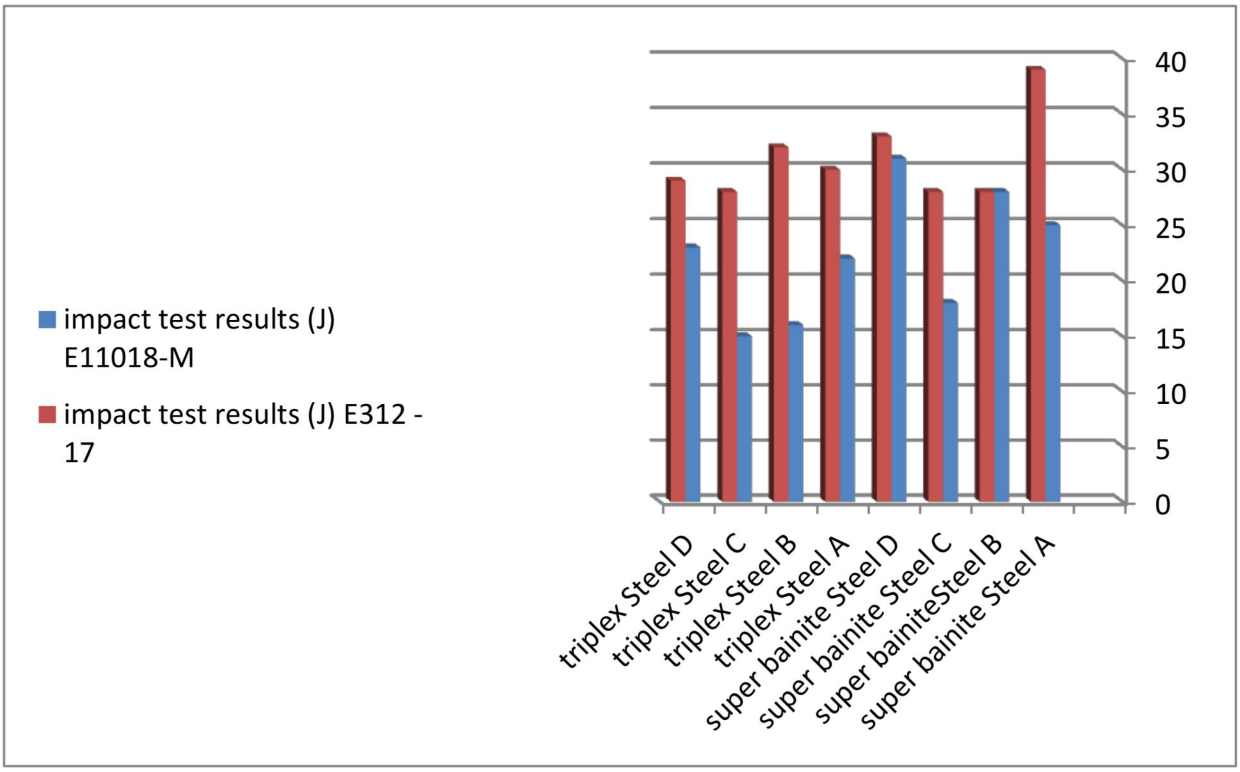

Figure 16: Histogram of V- notch impact tests values of welded joints super bainitic and triplex structure steels after welding using E11018-M and E312-17 electrodes

References

1. “Carbon Steel Handbook”, EPRI, Palo Alto, CA: (2007). 1014670.
2. B.S. Motagi, Ramesh Bhosle, “Effect of Heat Treatment on Microstructure and Mechanical Properties of Medium Carbon Steel”, International Journal of Engineering Research and Development, ISSN: 2278-067X, Volume 2, Issue 1 (July 2012), PP. 07-13.
3. H. K. D. H. Bhadeshia: “Bainite in steels”, 2nd edn; (2001), London, Institute of Materials.
4. Lihe Qian, Qian Zhou, Fucheng Zhang, Jiangying Meng, Ming Zhang, Yuan Tian, “Microstructure and mechanical properties of a low carbon carbide-free bainitic steel co-alloyed with Al and Si”, Materials and Design, 39 (2012) :264-268.
5. H Huang, MY Sherif, PEJ Rivera-Diaz-del-Castillo, “Combinatorial optimisation of carbide-free bainitic nanostructures”, Acta Materialia, 61 1639—1647 (2013).
6. Khare S, Lee K, Bhadeshia HKDH. Metall Trans A (2010); 41:922-928.
7. Guhui Gao a,n, Han Zhang b, Zhunli Tan c, Wenbo Liu a, Bingzhe Bai a,c, “A carbide-free bainite/martensite/austenite triplex steel with enhanced mechanical properties treated by a novel quenching–partitioning–tempering process”, Materials Science & Engineering, A559(2013): 169 -165.
8. G. Gomez, T. Perez, and H.K.D.H. Bhadeshia: Mater. Sci.Technol. 2009, vol. 25, pp. 1508–12.
9. G. Magudeeswaran, V. Balasubramanian, G.M. Reddy, andT.S.Balasubramanian: J. Iron. Steel Res. Int., 2008, vol. 15, pp. 87–94.2.
10. S.J. Alkemade: The Weld Cracking Susceptibility of High Hardness Armor Steel, Report # DSTO-TR-0320, Defence Science and Technology Organization, Edinburgh, 1996.
11. Krishna Murthy N. and Janaki Ram G.D.; Hot cracking behaviour of carbide-free bainitic weld metals; Mater. Design 92 (2016) 88-94.
12. Krishna Murthy N., Janaki Ram G.D., Murty B.S., Reddy G.M. and Rao T.J.P.; Carbide-free bainitic weld metal: A new concept in welding of armor steels; Metall. Mater. Trans. B 45 (2014) 2327-2337.

Authors

Sabry.M. AbdelAziz

Faculty of Industrial Education Department of Production Technology
eng.sabrimoussa@yahoo.com

M.A. Morsy

Central Metallurgical Research and Development Institute (CMRDI)
Morsy_abokhala@yahoo.com

Mohamed. K. El-Fawkhry

Central Metallurgical Research and Development Institute (CMRDI)
Mohamed.elfawkhry@gmail.com
